

Zero-Field Dichroism in the Solar Chromosphere

R. Manso Sainz¹ and J. Trujillo Bueno^{1,2}

¹*Instituto de Astrofísica de Canarias,
Vía Láctea s/n, E-38200 La Laguna, Tenerife, Spain*
²*Consejo Superior de Investigaciones Científicas*

(Dated: March 28, 2019)

Abstract

We explain the linear polarization of the Ca II infrared triplet observed close to the edge of the solar disk. In particular, we demonstrate that the physical origin of the enigmatic polarizations of the 866.2 nm and 854.2 nm lines lies in the existence of atomic polarization in their metastable $^2D_{3/2, 5/2}$ lower levels, which produces differential absorption of polarization components (dichroism). To this end, we have solved the problem of the generation and transfer of polarized radiation by taking fully into account all the relevant optical pumping mechanisms in multilevel atomic models. We argue that ‘zero-field’ dichroism may be of great diagnostic value in astrophysics.

Published in Physical Review Letters: Volume 91, Number 11, 111102, (2003)

PACS numbers: 95.30.-k, 95.30.Gv, 95.30.Jx, 32.80.Bx, 96.60.-j

Spectropolarimetry provides key information on the physical conditions and geometry of astrophysical plasmas otherwise unattainable via conventional spectroscopy [1]. The remote sensing of cosmical magnetic fields via the Zeeman effect is the most well-known example. In the presence of a magnetic field, the magnetic substates of atomic and molecular energy levels split, leading to a frequency shift of the σ^\pm ($\Delta M = \pm 1$) and π ($\Delta M = 0$) transitions [2]. If the Zeeman splitting is a significant fraction of the spectral line width, the polarization of the different components does not cancel out and an observable polarization pattern can then be produced via the emission process, as well as through dichroism and anomalous dispersion phenomena. The observed line polarization then depends on the strength and orientation of the magnetic field vector along the line of sight.

Yet there is a more fundamental mechanism producing linear polarization in spectral lines. In the outer layers of stellar atmospheres, where light escapes through the stellar surface, the atoms and molecules are illuminated by an anisotropic radiation field. The ensuing radiation pumping produces population imbalances among the magnetic sublevels of energy levels (that is, atomic polarization), in such a way that the population of substates with different values of $|M|$ are different. This is termed *atomic level alignment*. As a result, the emission process can generate linear polarization in spectral lines without the need for a magnetic field. This is known as scattering line polarization [2]. However, light polarization components *will also be differentially absorbed when the lower level of the transition is polarized* [3, 4]. Thus, the medium becomes dichroic simply because the light itself is escaping from it. Since this process has nothing to do with magnetic fields, we call it *zero-field dichroism*. This mechanism may be of great diagnostic value because in weakly magnetized astrophysical plasmas, like the ‘quiet’ solar atmosphere, the contribution of the transverse Zeeman effect to the linear polarization is normally negligible. In order for zero-field dichroism to be operative, the atomic polarization of the lower levels must survive depolarizing effects, such as those produced by elastic collisions. Moreover, weak magnetic fields modify the atomic level polarization via the Hanle effect [5, 6], where the magnetic field strength B (in gauss) that produces a significant change is $B \approx 1.137 \times 10^{-7} / (t_{\text{life}} g_L)$ (t_{life} and g_L being the level lifetime and Landé factor, respectively). Since the lifetimes of the lower levels of the transitions of interest are usually much larger than those of the upper levels, it is clear that diagnostic techniques based on this mechanism are sensitive to relatively low densities and magnetic field strengths.

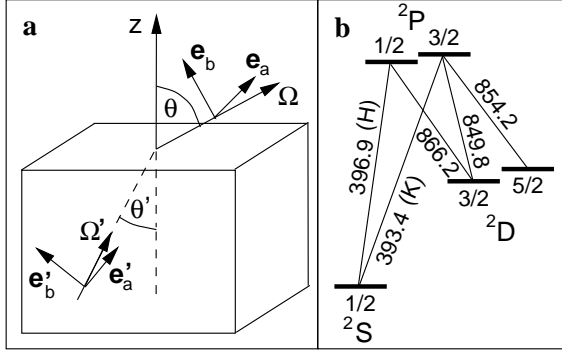


FIG. 1: (a) Scattering geometry. Ray propagating along the direction Ω with polar angle θ . The reference polarization direction for $Q > 0$ is along e_a , i.e., parallel to the stellar surface. (b) Grotrian diagram of our atomic model for Ca II indicating the total angular momentum of the levels and the spectral line wavelengths in nm.

In this letter, we demonstrate that zero-field dichroism is the key mechanism underlying the linear polarization of the Ca II infrared triplet detected in observations close to the edge of the solar disk, in very quiet regions far away from sunspots. The observed fractional polarization amplitudes of the Ca II lines at 849.8, 854.2 and 866.2 nm are $Q/I \approx 0.035\%$, 0.13% and 0.12%, respectively [7], the polarization signal in the 866.2 nm line being especially intriguing. This is a $^2D_{3/2} \rightarrow ^2P_{1/2}$ transition whose upper level ($^2P_{1/2}$) cannot be aligned. Therefore, emission following anisotropic radiative excitation cannot produce linear polarization in this spectral line and its detection has been considered ‘enigmatic’ [7].

Consider a plane-parallel stellar atmosphere without magnetic fields. For reasons of symmetry, choosing the reference polarization directions as in Fig. 1, the polarization state of a radiation beam can be described in terms of the intensity I and the Stokes parameter Q for linear polarization. The transfer of I and Q along a ray path element ds is described by the following equations:

$$\frac{d}{ds} I = \epsilon_I - \eta_I I - \eta_Q Q , \quad (1)$$

$$\frac{d}{ds} Q = \epsilon_Q - \eta_Q I - \eta_I Q , \quad (2)$$

where ϵ_I and ϵ_Q are the corresponding emissivities, while η_I and η_Q are the absorption and dichroism coefficients, respectively. In a spectral line, the emissivities depend on the excitation state of the upper level of the transition. Conversely, η_I and η_Q are given by the excitation state of the transition’s lower level. We have considered an additional contribution

to ϵ_I and η_I from a background continuum assumed to be unpolarized (i.e., η_I^{cont} and $\epsilon_I^{\text{cont}} = \eta_I^{\text{cont}} B_\nu$, B_ν being the Planck function), which is a very good approximation towards the red part of the solar spectrum (see [8]). For simplicity, we neglect stimulated emissions [15].

We choose the quantization axis for angular momentum along the Z-axis of Fig. 1. Since the radiation field is axially symmetric around this direction, no quantum interferences are induced between magnetic sublevels and the excitation state of each atomic level is fully described by the individual populations (occupation probabilities) N_M of each of its magnetic sublevels. Equivalently, we can describe the excitation state of each level of total angular momentum, J , by means of the following components of the atomic density matrix [9],

$$\rho_0^K(J) = \sum_{MM'} (-1)^{J-M} \sqrt{2K+1} \begin{pmatrix} J & J & K \\ M & -M' & 0 \end{pmatrix} N_M, \quad K = 0, 1, 2, \dots, 2J, \quad (3)$$

which are just linear combinations of N_M . Because the radiation field in the assumed model atmosphere has no net circular polarization, we have an internal symmetry in our problem: $N_M = N_{-M}$; therefore, only components ρ_0^K with K even can be different from zero. Of particular interest is ρ_0^0 , which is $(2J+1)^{-1/2}$ times the overall population of the level, and the alignment coefficient ρ_0^2 , which quantifies the population imbalance between the magnetic sublevels. The line emissivities can be expressed as [3, 10]

$$\epsilon_I^{\text{line}} = \epsilon_0 \rho_0^0 + \epsilon_0 w_{J_u J_\ell} \frac{1}{2\sqrt{2}} (3\mu^2 - 1) \rho_0^2, \quad (4)$$

$$\epsilon_Q^{\text{line}} = \epsilon_0 w_{J_u J_\ell} \frac{3}{2\sqrt{2}} (1 - \mu^2) \rho_0^2, \quad (5)$$

where the ρ_0^0 and ρ_0^2 values are those of the upper level of the line transition under consideration, $\mu = \cos \theta$ (see Fig. 1), and $\epsilon_0 = (h\nu/4\pi) A_{u\ell} \phi_\nu \mathcal{N} \sqrt{2J_u + 1}$ (where ν is the line frequency, $A_{u\ell}$ is the Einstein coefficient for the spontaneous emission process, \mathcal{N} is the total number of atoms per unit volume, and ϕ_ν is the absorption profile). $w_{J_u J_\ell}$ is a numerical coefficient whose value depends on the total angular momentum of the upper and lower levels, taking values $-2\sqrt{2}/5$, $\sqrt{2}/10$, and 0 for the lines at 849.8, 854.2, and 866.2 nm, respectively. On the other hand, η_I and η_Q are given by identical expressions, but using the ρ_0^0 and ρ_0^2 values of the lower level, $\eta_0 = (h\nu/4\pi) B_{\ell u} \phi_x \mathcal{N} \sqrt{2J_\ell + 1}$ instead of ϵ_0 (with $B_{\ell u}$ the Einstein coefficient for the absorption process), and $w_{J_\ell J_u}$ instead of $w_{J_u J_\ell}$, where the $w_{J_\ell J_u}$ values are $-2\sqrt{2}/5$, $\sqrt{7}/5$ and $\sqrt{2}/2$ for the aforementioned lines, respectively.

It can be deduced from Eqs. (1)-(2) and the expressions of $\epsilon_{I,Q}$ and $\eta_{I,Q}$, that the emergent fractional linear polarization at the core of a strong spectral line is approximately given by [4, 6]:

$$Q/I \approx \frac{3}{2\sqrt{2}}(1 - \mu^2)[w_{J_u J_\ell} \sigma_0^2(J_u) - w_{J_\ell J_u} \sigma_0^2(J_\ell)], \quad (6)$$

where $\sigma_0^2 = \rho_0^2/\rho_0^0$ is the fractional atomic alignment of the level under consideration. In this formula the σ_0^2 values are those at optical depth $\tau = \int \eta_I ds$ along the line of sight, where $\tau \approx 1$. Eq. (6) shows clearly that the observed fractional polarization in a given spectral line has in general two contributions, one from the atomic polarization of the upper level caused exclusively by emission from a polarized upper level ($\sigma_0^2(J_u)$), and another one from the atomic polarization of the lower level ($\sigma_0^2(J_\ell)$). As shown here, the latter one (caused by the selective absorption resulting from the population imbalances of the lower level) plays a key role in producing the linear polarization pattern of the Ca II IR triplet.

The atomic model in Fig. 1 is sufficiently realistic for modeling the Ca II infrared triplet. Since calcium has no hyperfine structure, the only levels that may carry atomic alignment are the upper level $^2P_{3/2}$ and the two metastable levels $^2D_{3/2,5/2}$. Therefore, nine density matrix elements are required to describe the atomic excitation: the overall population of each of the five levels (i.e., $\sqrt{2J+1}\rho_0^0(J)$), the atomic alignment of the two levels with $J = 3/2$, and the ρ_0^2 and ρ_0^4 values corresponding to the level with $J = 5/2$. These irreducible tensorial components of the atomic density matrix are governed by the statistical equilibrium equations, $0 = d\rho_Q^K(i)/dt = -\sum_{K'} R_{iKK'}\rho_0^{K'}(i) + \sum_{jK'} T_{jiKK'}\rho_0^{K'}(j)$, where the relaxation matrix has the three contributions $R_{iKK'} = \sum_\ell R_{i\ell KK'} + \sum_u R_{iuKK'} + D^K$ caused by decays toward lower levels, excitations towards upper levels, and depolarization by elastic collisions, respectively, while the transfer matrix has contributions caused by decays from upper levels ($T_{uiKK'}$) and excitations from lower levels ($T_{\ell iKK'}$) [10]. The relaxation rates read

$$R_{i\ell KK'} = \delta_{KK'} A_{i\ell} + \delta_{KK'} C_{i\ell}, \quad (7)$$

$$R_{iuKK'} = \delta_{KK'} B_{iu} J_0^0 + s_{KK'} B_{iu} J_0^2 + \delta_{KK'} C_{iu}, \quad (8)$$

and the transfer rates are

$$T_{uiKK'} = \sqrt{\frac{2J_u + 1}{2J_i + 1}} [\delta_{KK'} p_{K'} A_{ui} + \delta_{KK'} p_{K'} C_{ui}], \quad (9)$$

$$T_{\ell iKK'} = \sqrt{\frac{2J_\ell + 1}{2J_i + 1}} [\delta_{KK'} p_{K'} B_{\ell i} J_0^0 + q_{KK'} B_{\ell i} J_0^2 + \delta_{KK'} p_{K'} C_{\ell i}], \quad (10)$$

TABLE I: Numerical coefficients of Eqs. (7)-(10) calculated for the 5-level Ca II model of Fig. 1. $p_0 \equiv 1$ for all transitions. For the 396.9 nm line ($J_l = J_u = 1/2$) any other coefficients are zero.

line	p_2	q_{20}	q_{22}	s_{20}	s_{22}	s_{42}	s_{44}
393.4	—	$1/\sqrt{2}$	—	—	—	—	—
866.2	—	—	—	$1/\sqrt{2}$	—	—	—
849.8	$1/5$	$-2\sqrt{2}/5$	$-2\sqrt{2}/5$	$-2\sqrt{2}/5$	—	—	—
854.2	$\sqrt{14}/5$	$\sqrt{2}/10$	$2/(5\sqrt{7})$	$\sqrt{7}/5$	$\sqrt{2}/7$	$9\sqrt{6}/70$	$-\sqrt{2}/7$

where p , q , and s are numerical coefficients that depend only on the quantum numbers of the levels involved in the transition (see Table 1). Since the radiation field is axisymmetric the absorption rates depend only on the line-integrated mean intensity (J_0^0), and on

$$J_0^2 = \frac{1}{4\sqrt{2}} \int d\nu \int_{-1}^1 d\mu' \phi_\nu [(3\mu'^2 - 1)I + 3(1 - \mu'^2)Q].$$

It is important to note that in stellar atmospheres the polarization degree is small ($Q/I \ll 1$), and the main contribution to J_0^2 results from the intensity average. We call $\mathcal{A} = J_0^2/J_0^0$ the ‘degree of anisotropy’ of the radiation field. It determines the fractional atomic polarization that can be induced by optical pumping processes. In the solar atmosphere $\mathcal{A} \ll 1$, hence $\sigma_0^2 \ll 1$. Collisional rates C_{ij} due to collisions with an isotropic Maxwellian distribution of electrons are modeled in analogy to the excitation by an isotropic unpolarized radiation field. We have used the inelastic collisional rates for Ca II tabulated in [11], while the depolarizing rates $D^{(K)}$ due to collisions with neutral hydrogen atoms have been estimated according to Ref. [12].

Figure 2 shows results of the self-consistent solution of the radiative transfer and statistical equilibrium equations in a semi-empirical model [13] of the solar atmosphere. The numerical solution has been obtained applying the iterative methods outlined in Ref. [4]. The figure indicates how the degree of anisotropy corresponding to the K-line and to the 854.2 nm line vary with the K-line optical depth. These spectral lines are representative of the radiation fields in the UV doublet and IR triplet, respectively. The figure shows also the behavior of the fractional atomic alignments σ_0^2 of the 2nd, 3rd and 5th levels. Note that they have sizable values, even at the depths in the stellar atmosphere model where the line optical depths are unity along the line of sight.

The atomic alignment of the 5th level is governed by the radiation field in the K-line, with

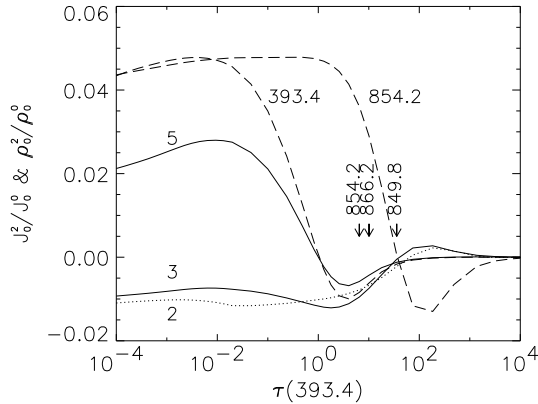


FIG. 2: Variation of ρ_0^2/ρ_0^0 in 2nd, 3rd and 5th levels of our Ca II model as a function of the K-line optical depth calculated along the vertical direction (solid and dotted lines). Dashed lines show J_0^2/J_0^0 in the K and 854.2 nm lines. Arrows indicate the layer in the FAL-C model atmosphere [13] where, for each of the three IR lines, $\tau = 1$ along the $\mu = 0.1$ line of sight.

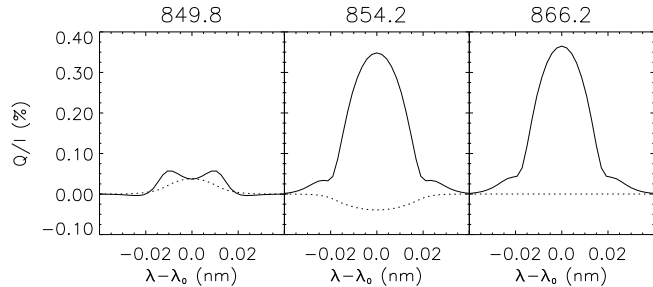


FIG. 3: Emergent fractional polarization of the Ca II infrared triplet at $\mu = 0.1$ in the FAL-C semi-empirical model of the solar atmosphere (solid lines). The shapes of the calculated Q/I profiles and their relative line-core amplitudes are in good agreement with the reported observations (see [7]). Dotted lines: Q/I profiles if the *long-lived* metastable $^2\text{D}_{3/2, 5/2}$ levels were completely unpolarized.

optical pumping in the lines at 849.8 nm and 854.2 nm playing only a marginal role. In fact, the height variation of $\sigma_0^2(5)$ closely follows that of the degree of anisotropy in the K-line throughout the whole atmosphere, with $\sigma_0^2(5) \approx \sqrt{2}/2 (J_0^2/J_0^0)(\text{K})$. On the other hand, there are two optical pumping processes able to introduce atomic alignment in the lower levels of the Ca II IR triplet (the metastable levels): *repopulation pumping*, which results from the spontaneous decay of the polarized 5th level; *depopulation pumping*, which occurs when

some lower state sublevels absorb anisotropic light more strongly than others. Since the infrared triplet lines are much weaker than the ultraviolet H- and K-lines ($\eta_I^{\text{line}}/\eta_I^{\text{cont}} \approx 10^5$ for the former, while $\eta_I^{\text{line}}/\eta_I^{\text{cont}} \approx 10^7$ for the latter lines), the IR line photons escape from deeper atmospheric regions, where the J_0^2/J_0^0 values of the IR line transitions are much larger than the (negligible) σ_0^2 value of the 5th level at such depths (see Fig. 2). Consequently, at such atmospheric depths the long-lived metastable levels 2 and 3 are mainly aligned by *depopulation pumping* rather than by spontaneous emission from the upper level with $J = 3/2$.

The solid lines in Fig. 3 show the emergent fractional polarization of the Ca II infrared triplet calculated at $\mu = 0.1$. Dotted lines show the emergent fractional polarizations if the metastable levels were unpolarized and dichroism negligible. Since the upper level of the 866.2 nm line cannot be aligned, the Q/I signal in this transition is exclusively caused by dichroism [see Eq. (6)]. The linear polarization observed in the 854.2 nm line can, in principle, be caused by both, the emission events from the polarized upper level and to the differential absorption by the polarized lower level. However, $|\sigma_0^2(^2\text{D}_{5/2})| > |\sigma_0^2(^2\text{P}_{3/2})|$ at $\tau(854.2) \approx 1$ (see Fig. 2), while $w_{J_\ell J_u} > w_{J_u J_\ell}$ in Eq. (6). Therefore, the observed Q/I signal is *de facto* also mainly caused by dichroism in the solar atmosphere. The 849.8 nm line forms significantly deeper in the solar atmosphere, where the fractional alignment of its upper and lower levels are close to zero, hence its much lower polarization signal, whose sign turns out to be very sensitive to the assumed atmospheric model.

Note that the calculated Q/I amplitudes of the 854.2 nm and 866.2 nm lines (see Fig. 3) are roughly twice the values reported in [7]. This can be due either to a simplified atmospheric modeling (the highly inhomogeneous solar atmosphere may not be well represented by a one-dimensional semi-empirical model), and/or to the existence of depolarizing mechanisms. Either case emphasizes the great diagnostic potential of the scattering polarization observed in the Ca II IR triplet. For example, collisional depolarizing rates five times larger than the nominal values used here only slightly affect the ensuing Q/I amplitudes. On the other hand, in the presence of a microturbulent magnetic field with a strength as low as 0.01 gauss, the atomic polarization of the metastable $^2\text{D}_{3/2,5/2}$ levels are significantly reduced and hence the emergent linear polarization in the 854.2 nm and 866.2 nm lines decreases to values similar to those observed (Hanle effect).

Zero-field dichroism may also be operating in other astrophysical objects (e.g., accreting

systems) and should be fully taken into account when interpreting spectropolarimetric observations in other spectral lines besides the Ca II IR triplet itself, whose polarization has been observed recently in supernovae [14].

Research partially funded by the Spanish Ministerio de Ciencia y Tecnología through project AYA2001-1649.

- [1] Reviews introducing the interest of spectropolarimetry in several fields of astrophysics appear in *Astrophysical Spectropolarimetry*, proceedings of the XII Canary Islands Winter School of Astrophysics, Puerto de la Cruz, Tenerife, Spain, 2000, edited by J. Trujillo Bueno, F. Moreno-Insertis, and F. Sánchez (Cambridge University Press, Cambridge, U. K., 2002).
- [2] J. O. Stenflo, *Solar Magnetic Fields: Polarized Radiation Diagnostics* (Kluwer Academic Publishers, Dordrecht, 1994).
- [3] J. Trujillo Bueno and E. Landi Degl'Innocenti, *Astrophys. J. Lett.* **482**, 183 (1997).
- [4] J. Trujillo Bueno, in *Solar Polarization*, proceedings of an international workshop held in Bangalore, Bangalore, 1998, edited by K. N. Nagendra & J. O. Stenflo (Kluwer Academic Publishers, Dordrecht, 1999), p. 73.
- [5] W. Hanle, *Z. Phys.* **30**, 93 (1924).
- [6] J. Trujillo Bueno, in *Astron. Soc. Pacific Conf. Ser.* **236**, *Advanced Solar Polarimetry. Theory, Observation and Instrumentation*, proceedings of the 20th NSO/Sacramento Peak Summer Workshop, Sunspot, New Mexico, 2000, edited by M. Sigwarth (Astron. Soc. Pacific, San Francisco, 2001), p. 161.
- [7] J. O. Stenflo, C. U. Keller, and A. Gandorfer, *Astron. Astrophys.* **355**, 789 (2000).
- [8] A. Gandorfer, *The Second Solar Spectrum* (vdf Hochschulverlag AG an der ETH, Zürich, 2000), Vol. 1.
- [9] A. Omont, *Prog. Quantum Electron.* **5**, 69 (1977).
- [10] E. Landi Degl'Innocenti, *Sol. Phys.* **85**, 3 (1983); **91**, 1 (1984).
- [11] R. A. Shine and J. L. Linsky, *Sol. Phys.* **39**, 49 (1974).
- [12] F. K. Lamb and D. ter Haar, *Phys. Rep.* **2C(4)**, 253 (1971).
- [13] J. M. Fontenla, E. H. Avrett, and R. Loeser, *Astrophys. J.* **377**, 712 (1991).
- [14] D. C. Leonard, A. V. Filippenko, R. Chornock, and R. J. Foley, *Publ. Astron. Soc. Pac.*

114, 1333 (2002); K. S. Kawabata *et al.*, *Astrophys. J. Lett.* **580**, 39 (2002); L. Wang *et al.*, *Astrophys. J.* (in press) [preprint arXiv:astro-ph/0303397, 2003].

[15] For a blackbody at the effective temperature of the Sun ($T \approx 5800$ K), the number of photons per mode even at 900 nm is $\bar{n} \approx 6 \times 10^{-2} \ll 1$, and stimulated emission can be safely neglected.